5.0 INELASTIC EFFECTS.

In the preceding paragraphs, elastic behavior was assumed. This assumption is sufficiently accurate for large classes of materials at relatively low temperature and stress levels.

At higher temperature and for higher stress levels, however, the divergence between the behavior of real solids and that of the ideal elastic solid increases and the elastic idealization becomes inadequate; the behavior of the real solid is then said to be inelastic. To predict the inelastic behavior of a solid under given thermal and loading conditions, it is necessary to generalize the stress-strain relationship. There are three types of approaches to this generalization, although the borderlines between them are not well defined.

1. The most basic studies of this problem make use of the concepts and methods of solid-state physics. In this approach, the microstructure of the material is taken into consideration and it is attempted to predict the mechanical behavior of materials from this information.

2. It is also possible to disregard the microstructure of the material and to regard it as a continuum; the general principles of mechanics and thermodynamics as applied to continua are then used to determine the forms of stress-strain relations which are compatible with these principles.

3. The most direct procedure is to postulate simple inelastic stress-strain relations; these define various ideal inelastic bodies which, though not

representing any actual materials, nevertheless incorporate in simple combinations some of the different types of inelastic phenomena, such as creep, relaxation, plastic flow, or work-hardening.

Although considerable progress has been made in methods 1 and 2, thus far only the third approach has yielded information of direct utility to the stress analyst. In this paragraph, inelastic stress-strain relations are discussed from the third of these viewpoints.

5.0.1 Creep.

Creep is the time-dependent deformation that occurs under stress. Creep is normally observed by placing a constant load on a specimen and measuring its deformation with time at a constant elevated temperature. The curve showing the deformation as a function of time is known as a creep curve. Creep curves obtained for various materials, temperatures, and stresses have certain common features, which are illustrated in Figure 5.0-1. These are:

1. From A to B, the specimen undergoes an initial, almost instantaneous, extension on loading.

2. From B to C, the specimen creeps at a rate that decreases with time (primary stage or transient creep).

3. From C to D, the specimen creeps at a rate that is nearly constant (secondary stage or viscous creep).

4. From D to E, the specimen creeps at a rate that increases with time (tertiary stage or accelerating creep).

5. At E, the specimen fractures.

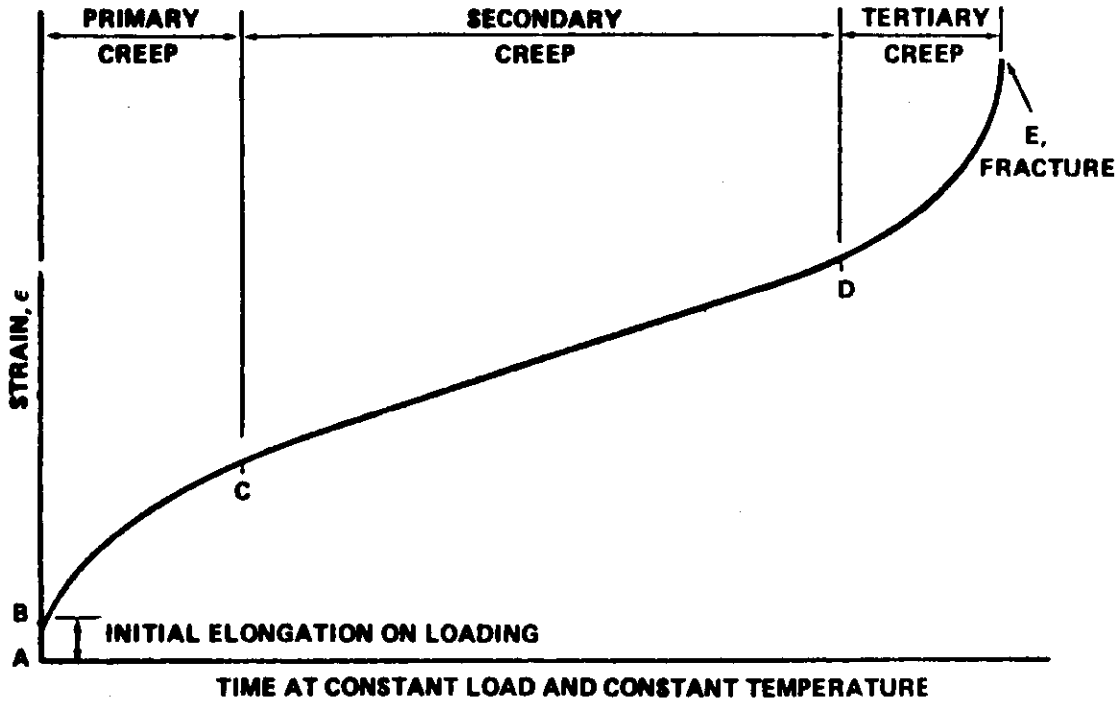

Figure 5.0-1. The idealized creep curve.

The rate of creep changes in the manner shown in Figure 5.0-2. During the secondary stage, the rate of creep drops to a minimum value that is approximately constant, as shown by the essentially straight line of the curve (refer to Fig. 5.0-1).

The primary stage of creep is a work- or strain-hardening stage, during which the resistance of the material to further creep is being built up by virture of its own deformation. For this reason, the rate of creep continually decreases. The secondary stage of creep (C-D) represents a balance between strengthening by work-hardening and weakening by thermal softening.

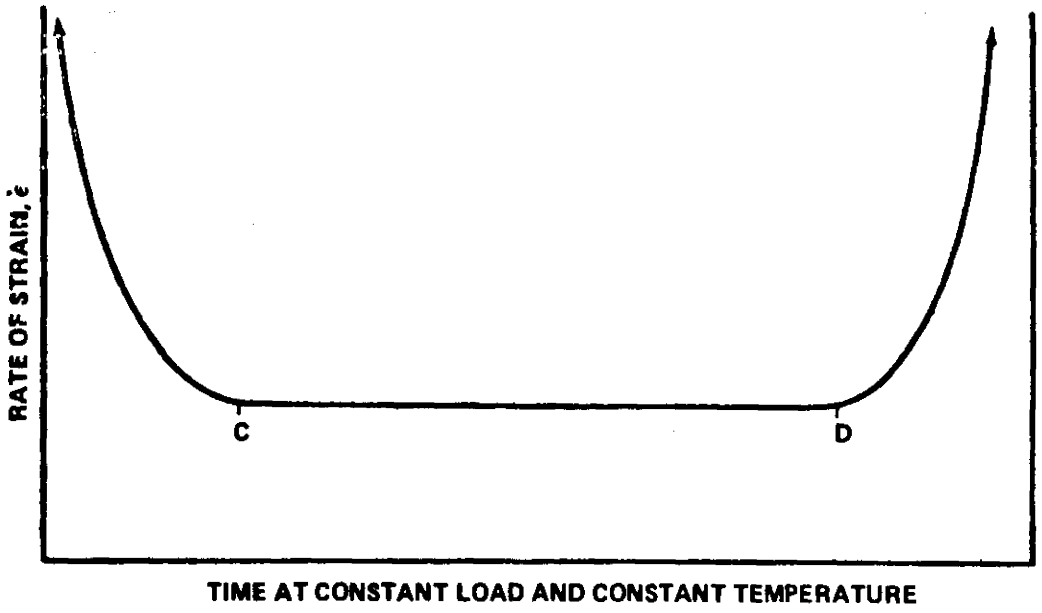

Figure 5.0-2. Variation in rate of creep with time.

The tertiary stage, or accelerating rate of creep immediately before fracture, is often caused by an increase in stress that accompanies the decrease in cross-sectional area of the specimen during creep under a constant load. This decrease in the load-carrying area may be due either to the decrease of the diameter of the specimen as it elongates or to the formation of intercrystalline cracks. These cracks can also act as stress-raisers. In other cases, the accelerating creep rate is due to a change in the metallurgical structure, such as recrystallization.

5.0.1.1 Design Curves.

For engineering purposes, the results of tests at various stresses and temperatures are summarized in more convenient form. Figure 5.0-3 shows

a plot that is most useful when the temperature and the lifetime of a part are fixed by the conditions of operation, and an allowable stress must be determined so that the part will not fracture or deform more than a certain amount during service. Having a set of these curves at the proper temperature, the designer can set off the lifetime along the abscissa and project it upwards; the intersection of this vertical line with the proper curve then determines the maximum allowable stress, and the design stress will be this quantity less a suitable factor of safety. Time and stress are usually plotted on logarithmic scales, where stress is the load divided by the original cross-sectional area. Frequently the data points on the rupture curves are identified with a number that gives the percent elongation, or reduction in area, at fracture; thus, some measurement of the ductility of the material is provided.

When the requirements are simply that a part must not fracture in service, and there are no limits on the amount of tolerable deformation, only the rupture curve in Figure 5.0-3 is needed. In such cases, the rupture curves for a number of temperatures can be collected on a single diagram, as in Figure 5.0-4, which is usually known as a "stress-rupture diagram." These curves show the variation in the time to fracture as a function of stress at several constant temperatures, and they are used in the same manner as the curves in Figure 5.0-3.

There are various ways of cross-plotting the previous figures. Plots of the stress versus temperature for lines of constant rupture life or constant

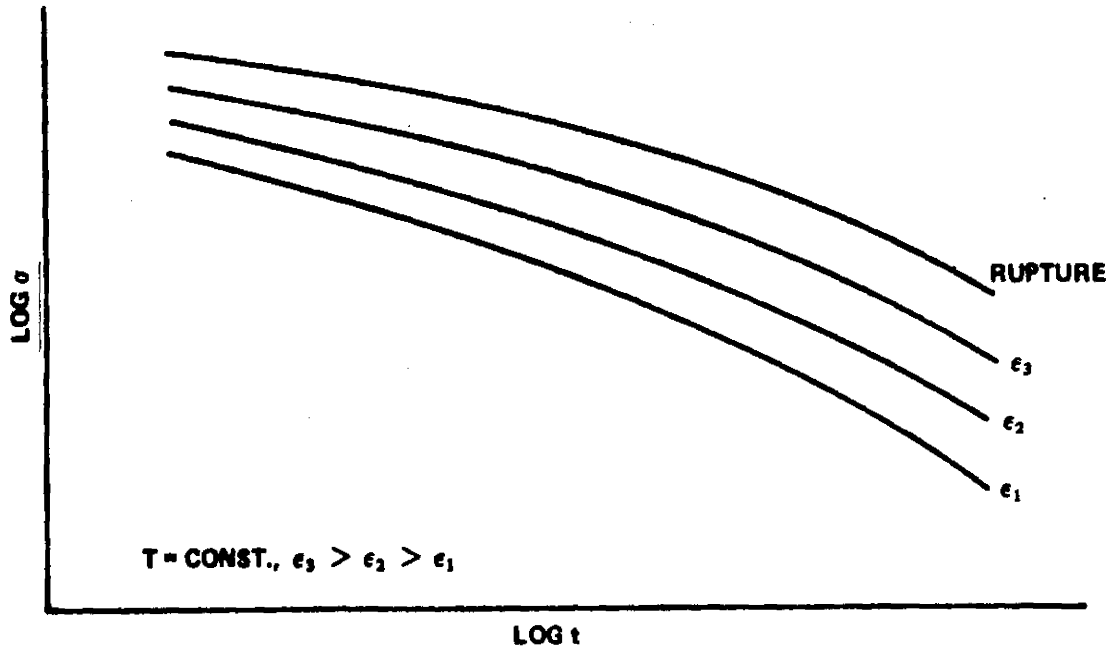

Figure 5.0-3. Schematic presentation of creep-rupture data showing effect of stress at constant temperature on the time to rupture or specific amounts of strain.

minimum creep rate are common. These curves are sometimes plotted on the same diagram with curves showing results from short-time tensile tests, as in Figure 5.0-5. Such diagrams give complete descriptions of the mechanical behavior over wide temperature ranges. At low temperatures, where creep is unimportant, designs are based on the results of short-time tensile tests; at higher temperatures, where the creep-rupture strength curves are below the tensile test curves, designs must be based on the creep-rupture behavior.

Curves of this type are readily available for most common metals in MIL-HDBK-5 [41].

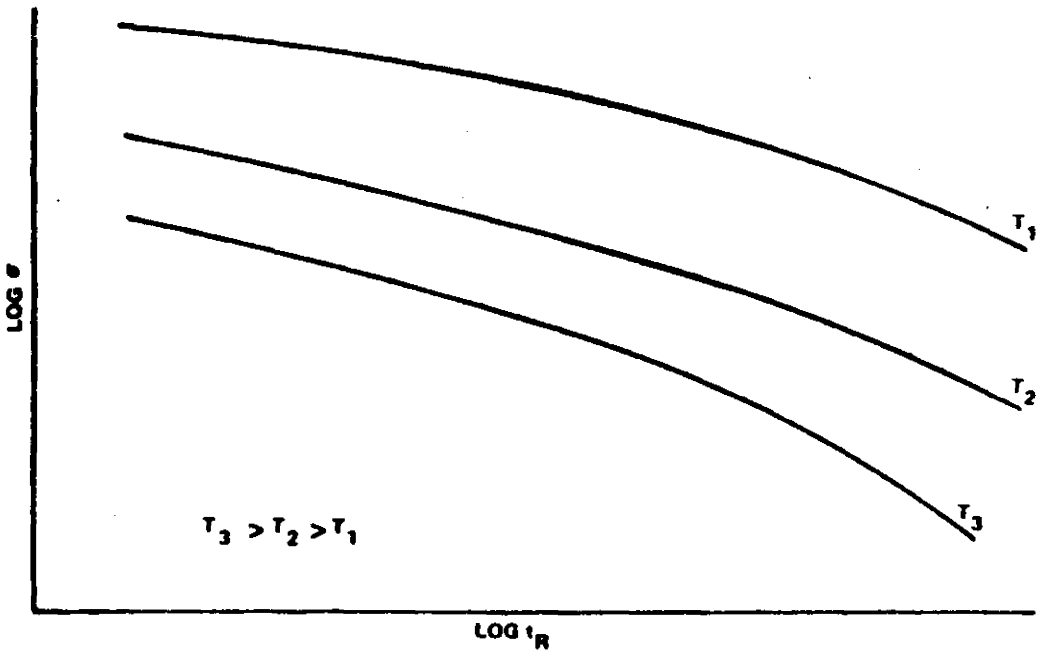

Figure 5.0-4. Schematic presentation of creep-rupture data showing effect of stress on the time to rupture at various temperatures.

5.0.1.2 Stress Relaxation.

Creep assumes a constant force; if, on the other hand, a bar is subjected to a constant elongation and the temperature is raised to a high level, with the elongation being maintained constant, the force required to produce this elongation will be observed to decrease continuously with time (Fig. 5.0-6). This mode of inelastic behavior is known as stress relaxation.

An important characteristic of both creep and stress relaxation is that time is required for their action. Thus, it may be expected that effects of this type will be unimportant for processes of relatively short duration.

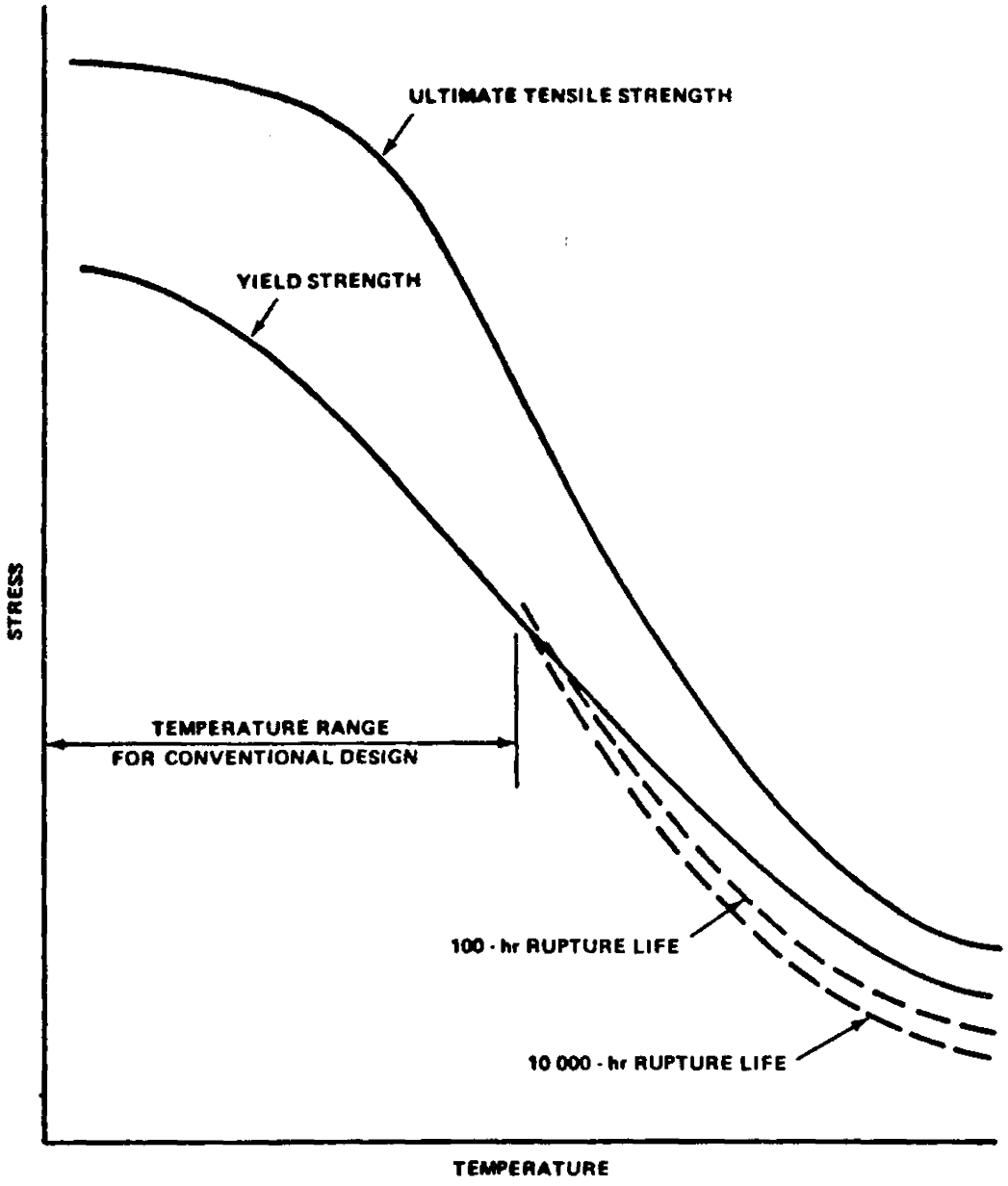

Figure 5.0-5. Schematic presentation of tensile and creep-rupture properties.

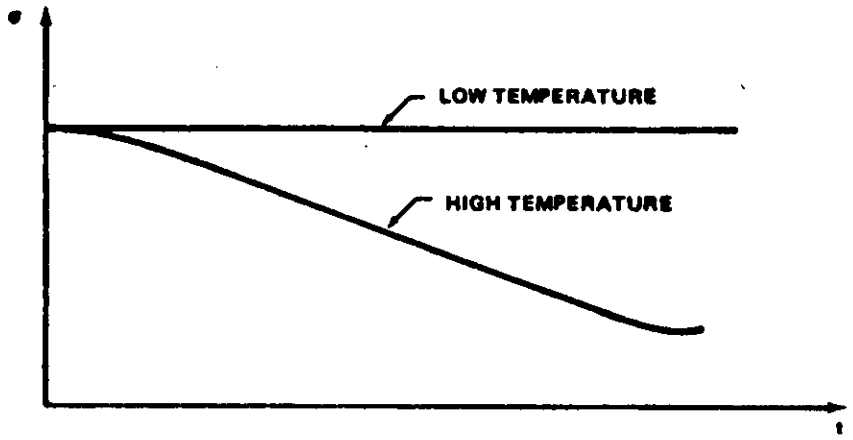

Figure 5.0-6. Stress relaxation under constant deformation.

5.0.2 Viscoelasticity.

Often, idealized bodies are defined which exhibit the characteristics of creep and stress relaxation. These idealized bodies take the form of simple mechanical models composed of springs and dashpots, whose deformation defines the stress-strain relationship for the given material. This approach is called viscoelasticity.

To represent the creep behavior of a material, many various mechanical models can be formulated composed of different combinations of springs and dashpots. Some of the more common ones can be found in Refs. 1 and 42.

5.0.3 Creep Buckling.

Consider a column under a constant axial compressive load; if the column is not perfectly straight initially (as is always the case because of unavoidable manufacturing inaccuracies), then some bending will occur. The

bending stresses are accompanied by a certain strain rate, which implies increasing deflections; these in turn cause higher stresses so that a self-excited or unstable situation arises. This process leads to collapse at a finite critical time and is known as creep buckling.

The following observations apply to creep buckling (Ref. 1):

1. The phenomenon of creep buckling is, both physically and mathematically, quite different from the usual type of buckling phenomenon. The usual buckling load represents a "point of bifurcation" on a load versus deflection plot, a point beyond which more than one equilibrium configuration is possible; creep buckling is characterized by deflections increasing beyond all bounds.

2. Mathematically, creep buckling can occur at a finite time only if the material follows a nonlinear creep law.

3. The column will undergo creep buckling at any value of the compressive axial load, no matter how small.

4. Creep buckling will occur whenever the column has initial imperfections, and only then.

5. The value of t_{cr} depends on the initial deflection and on the magnitude of the load; it has been found to be not too strongly affected by changes in the former but very sensitive to changes in the latter.

6. The small-deflection analysis is, of course, not valid in the immediate neighborhood of the critical time because the deflections are then

large. However, calculations based on a small-deflection theory are valid up to times very close to the critical; they thus cover, in effect, the entire range of practical interest.

5.0.3.1 Column of Idealized H-Cross Section.

The critical time for creep buckling to occur for a simply supported column of idealized H-cross section [two concentrated flanges, of area (A/2) each, at a distance h apart] is given by:

$$t_{cr} = k \log \left[1 + \left(\frac{4}{a_0^2} \right) \right]$$

where

$$k = \frac{1}{24} \left(\frac{\pi h}{L} \right)^2 \left(\frac{\lambda A}{P_0} \right)^3 ,$$

L = length of column ,

P_0 = column load,

a_0 = maximum value of initial imperfection,

and

λ = constant in the strain-stress relationship.

$$\frac{d\epsilon}{dt} = \left(\frac{\sigma}{\lambda} \right)^n .$$

5.0.3.2 Rectangular Column.

Analysis of the critical buckling time for rectangular columns is very difficult. A way of circumventing this difficulty has been established, whereby

upper and lower bounds for the critical time are obtained (t^*_{cr}) and are so designated by the use of an asterisk.

For a column with a rectangular cross section of height h and width b, subjected to an average stress $\sigma_0 = P_0/bh$ and obeying a stress-strain law of

$$\dot{E} = (\dot{\sigma}/E) = (\sigma/\lambda)^n \quad ,$$

upper and lower bounds for the nondimensional critical time t^*_{cr} are plotted in Figure 5.0-7 against the ratio (z_0/h) of the initial center-deflection to the height of the bar. For small values of this ratio (say $z_0/h < 0.015$) these bounds may be determined from the asymptotic expression

$$t^*_{cr} = \log \frac{h}{z_0} - c$$

with the values of the coefficient c listed in Table 5.0-1.

The spread between the bounds may be seen from Figure 5.0-7 to vary with the ratio z_0/h. However, from Ref. 1, if $\sigma_0/\sigma_E > 0.8$, then the lower bound will be a good approximation for t^*_{cr}, whereas if $\sigma_0/\sigma_E < 0.2$, the upper bound on t^*_{cr} will be a good approximation to the actual value of the critical time. $\left(\sigma_E = \text{Euler buckling stress} = \frac{\pi^2 E h^2}{12 L^2} \right)$.

5.0.3.3 Flat Plates and Shells of Revolution.

The method presented here may be used to predict critical conditions for the creep buckling of flat plates and shells of revolution which satisfy the following requirements:

TABLE 5.0-1. VALUES OF C

n	For Lower Bound	For Upper Bound
3	0.987	0.26
4	1.57	0.56
5	1.95	0.81
6	2.26	1.02
7	2.45	1.16

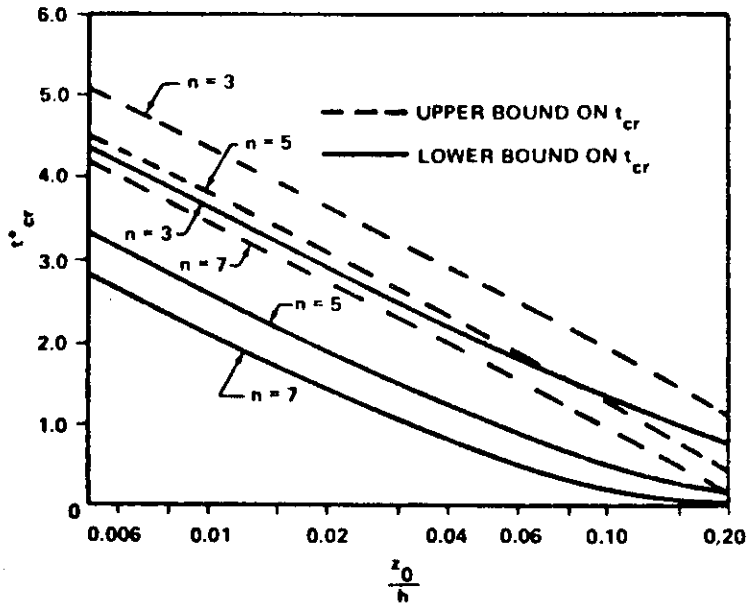

Figure 5.0-7. Upper and lower bounds for the critical time t^*_{cr} for creep buckling of a rectangular column.

1. The member is made of an isotropic material.

2. The stress intensity σ_i [see equations (1)] is uniform throughout the structure.

3. The configuration, boundary conditions, and type of loading are such that appropriate formulas are available for room-temperature values of both the critical stress intensity σ_i [see equations (1)] and the plasticity reduction factor.

Temperature Distribution.

It is assumed that the member is at a uniform elevated temperature.

Method.

The method presented here is essentially that which was published by Gerard in Ref. 43 and constitutes a classical stability approach based on the concepts set forth by Rabotnov and Shesterikov [44]. In Ref. 45, Jahsman and Field show comparisons of various theoretical predictions with column test data. The theory attributed there to Gerard is that of Ref. 46, which was published before Ref. 43 and has a different basis. On the other hand, the curves which Jahsman and Field [45] identify with the Rabotnov-Shesterikov label were developed from the method given in this paragraph. The aforementioned comparisons seem to indicate that this technique will give conservative predictions. However, this conclusion could possibly be because:

1. The test data were corrected to eliminate the effects of initial imperfections.

2. The analysis is concerned with the onset of instability, whereas the experimental data are for final collapse.

The presentation by Jahsman and Field includes plots obtained from each of three different theoretical approaches [43, 46, 47]. Of these, the approach of Ref. 43 gave the most conservative predictions. This is a desirable situation in view of the uncertainties associated with classical stability approaches to creep buckling problems. For one thing, this general theoretical concept ignores the detrimental effects from initial imperfections. However, to properly account for this influence, much more complicated methods would be required and these would not fall within the intended scope of this handbook. Therefore, in the procedure recommended below, an attempt is made at least to partially account for the imperfection effects in shells of revolution. This is done by the introduction of available room-temperature knockdown factors.

Recommended Procedure.

Obtain from the literature, or a suitable test program, a family of creep curves for specimens made of the desired material and subjected to unaxial loading while at the appropriate service temperature. These curves should be of the type shown in Figure 5.0-8 where σ_i and ϵ_i are the stress intensity and strain intensity, respectively, and are defined as follows for plane-stress conditions:

$$\sigma_i = \left(\sigma_x^2 + \sigma_y^2 - \sigma_x \sigma_y + 3\tau_{xy}^2\right)^{1/2}$$

and (1)

$$\epsilon_i = \frac{2}{\sqrt{3}} \left(\epsilon_x^2 + \epsilon_y^2 + \epsilon_x \epsilon_y + \frac{\gamma_{xy}^2}{4}\right)^{1/2} .$$

Using data obtained from these plots, create a family of curves similar to those of Figure 5.0-9 where $\dot{\epsilon}_i$ is the strain-rate intensity defined as follows for a state of plane stress:

$$\dot{\epsilon}_i = \frac{2}{\sqrt{3}} \left(\dot{\epsilon}_x^2 + \dot{\epsilon}_y^2 + \dot{\epsilon}_x \dot{\epsilon}_y + \frac{\dot{\gamma}_{xy}^2}{4} \right)^{1/2} . \tag{2}$$

The dots indicate differentiation with respect to time; for example,

$$\dot{\epsilon}_x^2 = \left(\frac{\partial \epsilon_x}{\partial t} \right)^2 . \tag{3}$$

The results embodied in Figure 5.0-9 are then used to develop still another family, which is illustrated in Figure 5.0-10. Following this, select appropriate formulations for conventional room-temperature values of both the critical stress intensity $(\sigma_i)_{cr}$ and the plasticity reduction factor η. For example, in the case of an axially compressed, moderate-length, circular cylinder, one obtains

$$(\sigma_i)_{cr} = \eta \, \Gamma \, \frac{Eh}{R\sqrt{3(1 - \nu_e^2)}} \tag{4}$$

and

$$\eta = \left(\frac{1 - \nu_e^2}{1 - \nu^2} \right)^{1/2} \frac{\sqrt{E_t E_s}}{E} \tag{5}$$

where Γ is the room-temperature knockdown factor and

$$\nu = 0.50 - \frac{E_s}{E} (0.50 - \nu_e) . \tag{6}$$

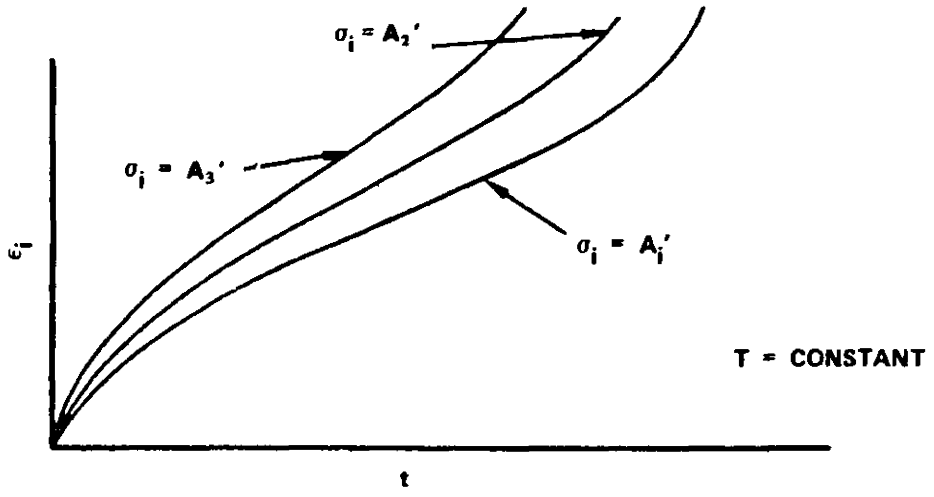

Figure 5.0-8. Constant-load creep curves.

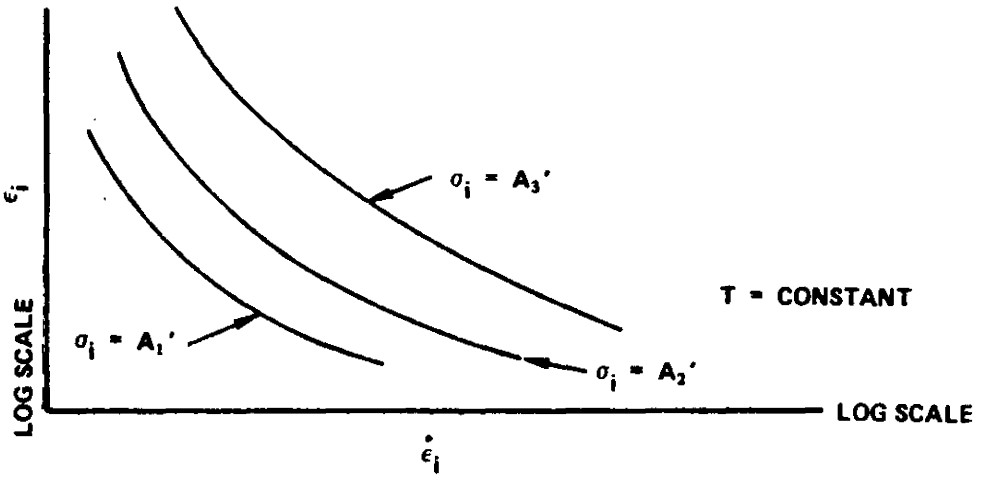

Figure 5.0-9. Curves derived from Figure 5.0-8.

Values for Γ may be obtained from Ref. 48 or other suitable sources. In addition, use the short-time elevated-temperature values for E and ν_e. On the other hand, the tangent and scant moduli (E_t and E_s, respectively) are those associated with the curves illustrated in Figure 5.0-10. Therefore,

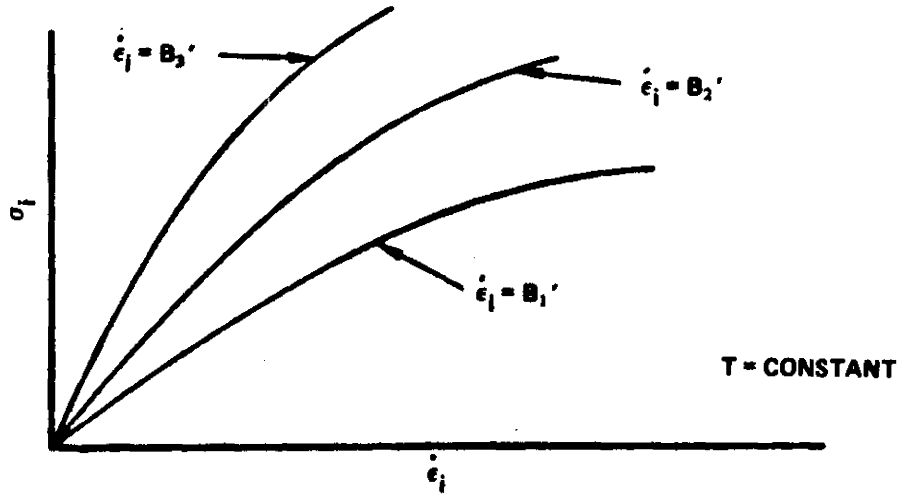

Figure 5.0-10. Curves derived from Figure 5.0-9.

working with this figure, proceed from left to right along the σ_i line corresponding to the applied load and use a trial-and-error procedure to determine the strain intensity ϵ_i at which

$$\text{applied } \sigma_i = \eta \ \Gamma \ \frac{Eh}{R\sqrt{3(1-\nu_e^2)}} \quad . \tag{7}$$

Following this, return to Figure 5.0-8 and establish the time t associated with this combination of σ_i and ϵ_i. This is the predicted time to the onset of creep buckling and can be denoted as t_{cr}.

Although the preceding presentation has dealt with the specific case of an axially compressed circular cylinder, it should be obvious that this method constitutes a general approach which can be used for the analysis of creep buckling in various types of plates and shells subjected to an assortment of loading conditions. It should be noted, however, that $\Gamma = 1.0$ for flat plates (and columns).